Eur J Nucl Med Mol Imaging (2017) 44:1647–1655
DOI 10.1007/s00259-017-3743-z

ORIGINAL ARTICLE

Early PET imaging with [68]Ga-PSMA-11 increases the detection rate of local recurrence in prostate cancer patients with biochemical recurrence

Christian Uprimny[1] · Alexander Stephan Kroiss[1] · Josef Fritz[2] · Clemens Decristoforo[1] · Dorota Kendler[1] · Elisabeth von Guggenberg[1] · Bernhard Nilica[1] · Johanna Maffey-Steffan[1] · Gianpaolo di Santo[1] · Jasmin Bektic[3] · Wolfgang Horninger[3] · Irene Johanna Virgolini[1]

Received: 7 April 2017 / Accepted: 24 May 2017 / Published online: 6 June 2017
© Springer-Verlag Berlin Heidelberg 2017

Abstract
Purpose PET/CT using ^{68}Ga-labelled prostate-specific membrane antigen PSMA-11 (HBEDD-CC) has emerged as a promising imaging method in the diagnostic evaluation of prostate cancer (PC) patients with biochemical recurrence. However, assessment of local recurrence (LR) may be limited by intense physiologic tracer accumulation in the urinary bladder on whole-body scans, normally conducted 60 min post-tracer injection (p.i.). It could be shown on early dynamic imaging studies that ^{68}Ga-PSMA-11 uptake in PC lesions occurs earlier than tracer accumulation in the urinary bladder. This study aims to investigate whether early static PET acquisition increases detection rate of local recurrence on ^{68}Ga-PSMA-11 PET/CT in comparison to PET imaging 60 min p.i..
Methods 203 consecutive PC patients with biochemical failure referred to ^{68}Ga-PSMA-11 PET/CT were analysed retrospectively (median prostate specific antigen (PSA) value: 1.44 ng/ml). In addition to whole-body PET/CT scans 60 min p.i., early static imaging of the pelvis was performed, starting at a median time of 283 s p.i. (range: 243–491 s). Assessment was based on visual analysis and calculation of maximum standardized uptake value (SUV_{max}) of pathologic lesions present in the pelvic area found on early PET imaging and on 60 min-PET scans.
Results 26 patients (12.8%) were judged positive for LR on PET scans 60 min p.i. (median SUV_{max}: 10.8; range: 4.7–40.9), whereas 50 patients (24.6%) revealed a lesion suggestive of LR on early PET imaging (median SUV_{max}: 5.9; range: 2.9–17.6), resulting in a significant rise in detection rate ($p < 0.001$). Equivocal findings on PET scans 60 min p.i. decreased significantly with the help of early imaging (15.8% vs. 4.5% of patients; $p < 0.001$). Tracer activity in the urinary bladder with a median SUV_{max} of 8.2 was present in 63 patients on early PET scans (31.0%). However, acquisition starting time of early PET scans differed significantly in the patient groups with and without urinary bladder activity (median starting time of 321 vs. 275 s p.i.; range: 281–491 vs. 243–311 s p.i.; $p < 0.001$). Median SUV_{max} value of lesions suggestive of LR on early images was significantly higher in comparison to gluteal muscle, inguinal vessels and seminal vesicle/anastomosis (median SUV_{max}: 5.9 vs. 1.9, 4.0 and 2.4, respectively).
Conclusions Performance of early imaging in ^{68}Ga-PSMA-11 PET/CT in addition to whole-body scans 60 min p.i. increases the detection rate of local recurrence in PC patients with biochemical recurrence. Acquisition of early PET images should be started as early as 5 min p.i. in order to avoid disturbing tracer activity in the urinary bladder occuring at a later time point.

Keywords ^{68}Ga-PSMA-11 PET/CT · Prostate canceer · Biochemical relapse · Local recurrence · Early PET imaging

✉ Christian Uprimny
christian.uprimny@tirol-kliniken.at

[1] Department of Nuclear Medicine, Medical University Innsbruck, Anichstrasse 35, 6020 Innsbruck, Austria

[2] Department of Medical Statistics, Informatics and Health Economics, Medical University Innsbruck, Innsbruck, Austria

[3] Department of Urology, Medical University Innsbruck, Innsbruck, Austria

Introduction

Radical prostatectomy (RP) and primary radiotherapy are treatment options with potentially curative intent in patients

with clinically localized prostate cancer (PC) [1, 2]. In up to 50% of patients biochemical recurrence (BR) after RP occurs, defined as serum prostate specific antigen (PSA) levels >0.2 ng/ml [3, 4]. Available imaging modalities do have limitations in the visualization of the site of tumour recurrence, especially at low PSA values [4–6]. The efficacy of salvage radiotherapy depends on early detection of LR when relapsing disease is still limited to the prostatic fossa [4, 7]. Magnetic resonance imaging (MRI) has proven to be a sensitive method in detecting LR, whereas its role in the diagnosis of metastases is restricted [5, 8]. Whole-body PET imaging with C-11- or F-18-labelled choline has been widely applied for assessment of BR [9, 10]. Unfortunately, choline PET lacks diagnostic accuracy in this indication and is inferior to MRI in the detection of LR [11–14]. Over the past few years, PET/CT with the ^{68}Ga-labelled prostate specific membrane antigen (PSMA) ligand Glu-urea-Lys(Ahx)-HBED-CC (PSMA-11), a ligand that binds to the cell-surface protein PSMA with overexpression on most PC, has been successfully introduced in the diagnostic work-up of PC patients [15–17]. Concerning the overall detection rate in BR, ^{68}Ga-PSMA-11 PET outperforms ^{18}F–choline PET [18–20].

In ^{68}Ga-PSMA-11 PET/CT, a whole-body scan starting 60 min post-tracer injection (p.i.) is usually performed in the clinical routine [17, 21, 22]. Due to high physiologic urinary bladder activity at this time point, identification of LR may be hampered in ^{68}Ga-PSMA-11 PET/CT [21, 23, 24]. It has been demonstrated that the application of early dynamic imaging in the first 8 min p.i. enables distinguishing tumour from bladder activity in ^{68}Ga-PSMA-11 PET/CT [25]. Tumour-related ^{68}Ga-PSMA-11 uptake occurs earlier than tracer accumulation in the urinary bladder and, therefore, LR might be easier to identify within the first minutes p.i. in comparison to PET scans 60 min p.i. [25].

As performance of early dynamic imaging is quite demanding, the primary goal of this study was to evaluate whether a single early static PET scan of the pelvic area could increase diagnostic performance of ^{68}Ga-PSMA-11 PET/CT in detecting LR in PC patients with biochemical relapse.

Materials and methods

Patients

203 consecutive PC patients with BR after definitive primary therapy referred to our department for a ^{68}Ga-PSMA-11 PET/CT from October 2014 to June 2016 were retrospectively analysed. In 179 patients, radical prostatectomy was performed as primary therapy, whereas 25 patients had received primary radiotherapy. Patients presented with a median PSA value of 1.44 ng/ml (range: 0.14–96.00). 41 patients (20.2%) showed a PSA value ≤0.5 ng/ml, whereas in 72 patients (35.5%), the PSA level was ≤1.0 ng/ml. Detailed patient characteristics are shown in Table 1.

Radiopharmaceutical

PSMA-11 [Glu-NH-CO-NH-Lys(Ahx)-HBED-CC; HBED-CC = *N,N′*-bis[2-hydroxy-5-(carboxyethyl)benzyl] ethylenediamine-N, N′-diacetic acid] was obtained from ABX Advanced Biochemical Compounds (Radeberg, Germany) of good manufacturing practice (GMP) quality. ^{68}Ga-PSMA-11 was prepared on an automated synthesis module (ModulaR-Lab PharmTracer; Eckert & Ziegler, Berlin) using a procedure previously described [25, 26]. The radiochemical purity of the final product was >91% as analysed by reversed-phase high-performance liquid chromatography and thin layer chromatography.

Imaging protocol

^{68}Ga-PSMA-11 PET/CT imaging was performed in a dual-phase mode using a dedicated PET/CT system (Discovery 690; GE Healthcare, Milwaukee, WI, USA). The acquisition protocol included an early static image of the pelvis centred on the prostate bed (one bed position with an axial field of view of 15.6 cm). After a fasting period of at least 6 h, patients were injected a median activity of 150 MBq ^{68}Ga-PSMA-11 (range 95–190 MBq). Variation of injected ^{68}Ga-PSMA-11 activity was due to the short half-life of ^{68}Ga and variable elution efficiencies of the ^{68}Ge/^{68}Ga radionuclide generator. Nevertheless, image quality of PET scans in patients in whom lower activities were administered was good and judged sufficient for correct image analysis. Early PET imaging was performed after positioning the patient on the bed of the PET scanner at a median acquisition starting time of 283 s (sec) p.i. (range: 243–491 s) with a duration of PET emission of two min. For attenuation correction and anatomic localisation, a low-dose CT of the same region was done before PET acquisition. 60 min after tracer injection, a whole-body PET/CT scan (skull base to upper thighs) in three-

Table 1 Patient characteristics

Patients	203
Primary radical prostatectomy	178
Primary radiation therapy	25
Age (years): median (range)	68 (54–92)
Initial Gleason score median (range)	7 (6–10)*
PSA (ng/ml): median (range)	1.44 (0.14–96.0)**
Salvage radiotherapy	62

*In 67 of 203 patients, no initial Gleason score could be obtained

**In 18 of 203 patients, no PSA within 4 weeks before PET scan was available

dimensional mode was conducted (emission time: 2 min per bed position, axial field of view: 15.6 cm per bed position). In 102 patients (50.2%), a diagnostic contrast-enhanced CT (ceCT) scan was performed. The ceCT scan parameters using "GE smart mA dose modulation" were: 100–120 kVp, 80–450 mA, noise index 24, 0.8 s per tube rotation, slice thickness 3.75 mm and pitch 0.984. A CT scan of the thorax, abdomen and pelvis (shallow breathing) was acquired 40–70 s after injection of contrast agent (60 to 120 ml of Iomeron 400 mg/l, depending on patient body weight), followed by a CT scan of the thorax in deep inhalation. In the remaining 101 patients, a low-dose CT scan was performed for attenuation correction of the PET emission data. The low-dose CT scan parameters using "GE smart mA dose modulation" were: 100 kVp, 15–150 mA, noise index 60, 0.8 s per tube rotation, slice thickness 3.75 mm and pitch 1.375. Reconstruction was performed with an ordered subset expectation maximization algorithm (OSEM) with four iterations per eight subsets.

Image analysis

All ^{68}Ga-PSMA-11 PET/CT images were analysed with dedicated commercially available software (GE Advance Workstation SW Version AW4.5 02), which allowed the review of PET, CT and fused imaging data in axial, coronal and sagittal slices. PET images were interpreted independently by two board-approved nuclear medicine physicians with more than 10 years of clinical experience.

Whole-body PET/CT images 60 min p.i. were evaluated with respect to LR, malignant lymph node (LN) involvement and distant metastases. Any focal uptake higher than surrounding background activity that did not correspond to physiologic tracer accumulation was considered pathologic and suggestive of malignancy. This interpretation criteria is the result of our clinical experience and goes in line with published literature [15–17, 21]. With regard to assessment of LR, only lesions with increased uptake at a typical area of local relapse that was clearly distinguishable from urinary bladder activity were counted as pathologic and rated as LR. In contrast, uncertain findings that could represent LR, but because of its localisation, could also be explained by urinary activity were considered as abnormal; however, they were not classified as pathologic (e.g. tracer accumulation in the midline adjacent to the urinary bladder). For analysis, equivocal findings were counted as negative for LR. In addition, semiquantitative analysis of all lesions visually considered typical for malignancy was performed using the maximum standardized uptake value (SUV_{max}). For SUV_{max} , calculation volumes of interest were drawn automatically with a manually adapted isocontour threshold centred on lesions with focally increased uptake. Furthermore, it was assessed if the so called "halo artefact" around the urinary bladder could be observed on PET scans 60 min p.i., an artefact due to high urinary bladder activity causing elimination of the PET signal around the urinary bladder [21, 27]. SUV_{max} measurement of the urinary bladder activity was performed in all patients.

In a second step, early PET images fused with low-dose CT were analysed. For assessment of LR, each lesion with focally increased uptake at a typical site of LR outside the urinary bladder was counted as suggestive of LR. As to evaluation of malignant LN involvement and bone metastases, early PET images were compared to the PET/CT images 60 min p.i. Only pathologic lesions that were present on whole-body PET and within the field of view of the early PET scans were assessed and analysed semiquantitatively. The urinary bladder was evaluated as to whether physiologic urinary activity was present at early imaging. SUV_{max} was calculated within volumes of interest that were placed over the sites of pathologic tracer accumulation consistent with tumour lesions (LR, LN, bone). SUV_{max} was measured in the urinary bladder of all patients in whom urinary activity was found, and in reference tissues such as inquinal vessels, gluteal muscle, and normal tissue in prostate bed/vesicourethral anastomosis/seminal vesicles. The latter served as a negative control group. It was chosen because the majority of LR occurs at this site; only regions with no apparent pathology were included in SUV_{max} measurements. Regarding detection rate of LR on early PET, analysis was performed in all patients investigated and in a subgroup comprising only patients in whom urinary bladder activity was absent.

Statistical analysis

Detection rates of LR on PET scans 60 min p.i. vs. early static PET scans were tabulated in cross-tables and compared with McNemar's test for paired observations. For quantitative variables, due to skewed distributions, we used rank-based nonparametric statistical tests: Wilcoxon signed rank-sum tests for paired observations for comparison of SUV_{max} values in various tissues and over time points; and Mann–Whitney U tests for comparison of SUV_{max}, PSA values and starting time of early static PET scan between various independent subgroups (e.g. PET-positive vs. PET-negative patients). A significance level of $\alpha = 0.05$ (two-tailed) was applied. Statistical analyses were performed using SPSS, version 22.0 (IBM Corp., Armonk, NY, USA).

Results

PET/CT studies 60 min p.i.

126 out of 203 patients showed at least one lesion with pathologic tracer accumulation consistent with tumour relapse on PET scans 60 min p.i., yielding an overall detection rate of 62.1%. Pathologic lesions consistent with malignant LN

involvement were found in 81 patients (39.9%), and pathologic foci suggestive of distant metastases could be detected in 35 patients (17.2%). The majority of distant metastases were confined to the bone; in three patients, ^{68}Ga-PSMA-11-positive lung metastases were present.

With regard to detection of LR, 26 patients (12.8%) were judged positive for LR on images 60 min p.i. 145 patients (71.4%) were clearly negative for LR on images 60 min p.i., whereas 32 patients (15.8%) showed an equivocal finding, classified as abnormal or uncertain but not as pathologic, as the findings were not definitely consistent with LR. Most of these cases represented tracer accumulation in the midline that was not discernable from intense physiologic urinary activity in the bladder or proximal urethra. Median SUV_{max} of urinary bladder activity 60 min p.i. measured in all patients was 61.3 (range: 10.7–172.2). The "halo artefact" could be found in 26 patients (12.8%). The median SUV_{max} value of all lesions indicative of LR 60 min p.i. was 10.8 (range: 4.7–40.9).

Early PET/CT studies

On early images, lesions with increased tracer accumulation highly suggestive of LR were found in 50 patients (24.6%), resulting in a significantly higher detection rate of LR compared to PET acquisition 60 min p.i. (24.6% vs. 12.8%; $p < 0.001$). An example of a patient in whom a LR is clearly visible on early PET is given in Fig. 1, whereas on PET images 60 min p.i., it is not distinguishable from the urinary bladder. All pathologic lesions classified as LR on images 60 min p.i. were also positive on early PET acquisition. Regarding LR, equivocal findings were present in only 9 patients (4.5%), resulting in a significant reduction of unclear cases in comparison to 60 min p.i. (15.8% vs. 4.5%; $p < 0.001$), as presented in Table 2. The majority of the 32 cases classified as equivocal on PET scans 60 min p.i. were not interpreted as pathologic on early PET ($n = 23$; 71.9%), most likely representing urinary activity. Seven unclear cases 60 min p.i. (21.9%) were regarded as positive for LR on early PET images, whereas two (6.2%) remained equivocal on early scans. In contrast, 7 patients with unclear findings on early PET were judged negative for LR on PET 60 min p.i. Figure 2 shows a case with an equivocal finding on the PET scan 60 min p.i. with no increased tracer uptake at that site on early PET, rendering an LR unlikely. Median SUV_{max} of all 50 lesions suggestive of LR on early imaging was 5.9 (range: 2.9–17.6).

In a subanalysis comprising all patients who only received radiotherapy as primary treatment ($n = 25$), 7 patients were judged positive for LR on PET 60 min p.i. compared to 9 on early PET. Equivocal findings were present in 7 patients 60 min p.i. and in 5 patients on early PET images.

Semiquantitative evaluation of reference tissues on early PET acquisition measured in the gluteal muscle, in the seminal vesicle/anastomosis and in inguinal vessels revealed a median SUV_{max} value of 1.9 (range: 1.1–3.3), 2.4 (range: 1.1–3.6) and 4 (range: 1.9–7), respectively. These values were significantly lower than median SUV_{max} in lesions suggestive of LR ($p < 0.001$). Nevertheless, an overlap in SUV_{max} values between malignant lesions and reference tissues was found, which was more pronounced in the area of inguinal vessels in contrast to gluteal muscle and the region of anastomosis/seminal vesicle. Table 3 shows the detailed SUV_{max} analysis of the LR-indicative lesions in comparison to SUV_{max} values of reference tissues.

Tracer accumulation in the urinary bladder was present in 63 patients (31.0%) on early PET images with a median SUV_{max} of 8.2 (range 3.0–45.8). In contrast, the median SUV_{max} value of the urinary bladder 60 min p.i. of these patients was 65.6 (range: 10.7–168.4). Image acquisition for early PET scans in patients in whom urinary bladder activity was already present on early PET acquisition was started significantly later, compared to those with no tracer accumulation in the urinary bladder on early images, with a median starting time of 321 s vs. 275 s, respectively (range: 281–491 s vs. 243–311 s; $p < 0.001$).

Furthermore pathologic lesions consistent with metastases on whole-body PET/CT scans 60 min p.i. were analysed on early PET images with regard to detectability and intensity of tracer uptake. A total of 128 metastases indicative of lesions in 80 patients (LNs: $n = 100$; bone: $n = 28$) could be identified in the pelvic region on PET scans 60 min p.i. 82 out of 100 LN present on images 60 min p.i. (82%) also showed a tracer accumulation on early images that exceeded tracer uptake of surrounding tissue, exhibiting a median SUV_{max} of 7.8 on early PET (range: 2.9–46.2), compared to a median SUV_{max} of 10.0 on the scans 60 min p.i. (range: 3.9–88.8). The remaining 18 LNs were not clearly visible on early images as they were obscured by adjacent vessel activity (mostly in the iliacal region). As to bone metastases, 27 out of 28 lesions (96.4%) with pathologic tracer uptake 60 min p.i. were also identified on early imaging, demonstrating a median SUV_{max} of 8.9 on early scans (range: 2.1–41.7) compared to a median SUV_{max} of 11.4 (range: 2.2–50.3) on images 60 min p.i. SUV_{max} values of all tumour lesions measured on early PET and PET scans 60 min p.i. are listed in Table 4. The majority of bone lesions rated positive on PET scans corresponded to sclerotic alterations on CT consistent with bone metastases (96.4%); one pathologic focal skeletal uptake did not show a correlate on CT.

In order to exclude possibly false positive findings on early PET imaging due to urinary bladder activity, a subgroup analysis of all patients with absent bladder activity on early PET images was performed ($n = 140$). In this subgroup, a lesion with pathologic ^{68}Ga-PSMA-11 accumulation typical for LR was found in 19 patients (13.6%) on the PET/CT scans 60 min p.i., whereas on early images, 39 patients (27.9%) were judged positive for LR, resulting in a significantly higher

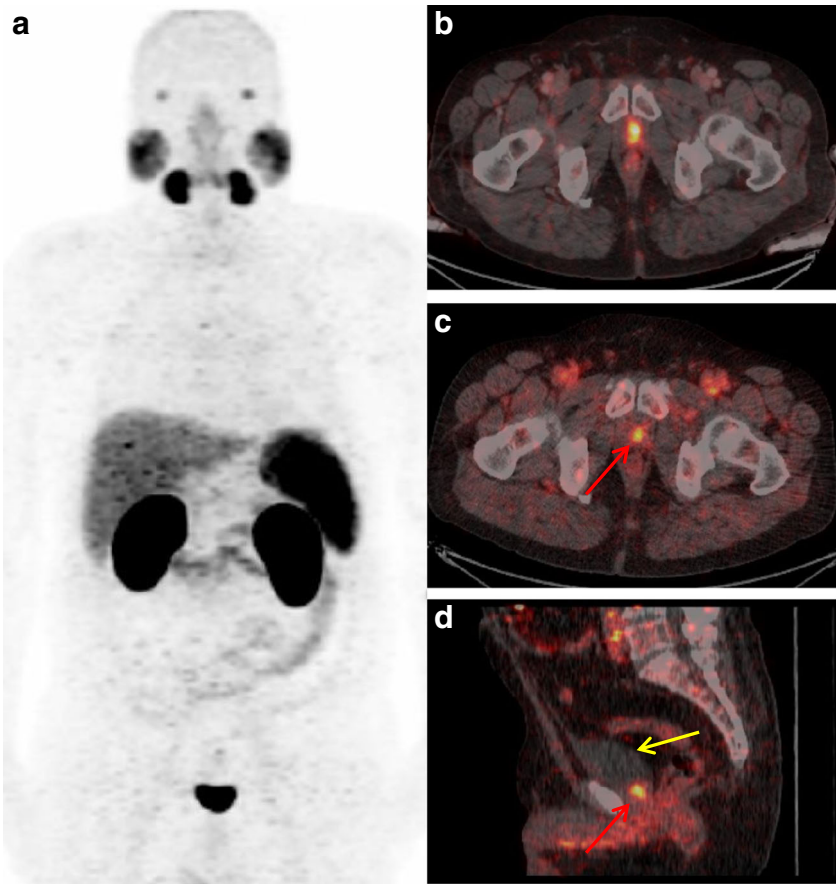

Fig. 1 ^{68}Ga-PSMA-11 PET/CT of a 67-year-old prostate cancer patient with biochemical recurrence after radical prostatectomy (PSA at PET time: 0.4 ng/ml), showing an intense focal tracer accumulation at the vesicourethral anastomosis with no clear distinction from urinary bladder activity on PET scan 60 min p.i., as seen on maximum intensity projection (MIP; **a**) and fused axial PET/CT (**b**) images. On fused axial (**c**) and sagittal (**d**) images of early PET/CT, a lesion with intense tracer uptake is present at the corresponding region (*red arrow*) with no tracer uptake visible in the urinary bladder (*yellow arrow*), a finding most likely representing local relapse of prostate cancer

detection rate ($p < 0.001$). In contrast to 23 patients with unclear findings concerning LR on PET images 60 min p.i. (16.4%), no equivocal finding was described on early PET scans, yielding a significant reduction ($p < 0.001$), as demonstrated in Table 2.

With respect to PSA levels, patients with lower PSA values were more likely to be judged positive for LR only on early PET. Median PSA value in patients regarded positive for LR only on early PET was significantly lower than in patients with LR-suggestive findings on both early PET and PET images 60 min p.i. (2.02 vs. 4.59 ng/ml; $p = 0.006$).

Regarding verification of lesions with pathologic tracer accumulation suspicious of LR on ^{68}Ga-PSMA-11 PET/CT, no histologic confirmation was available, mostly due to practical reasons. In addition, as patients were referred to us from many different urological practices and hospitals, information on follow-up of patients could not always be obtained. However, in 26 out of all 50 cases judged positive for LR (52%) the PET-positive lesion either showed a correlate on morphologic imaging (ceCT and/or subsequent MRI) or was confirmed on follow-up ^{68}Ga-PSMA-11 PET/CT. In 5 patients (10%), salvage RT to the prostatic fossa led to a drop of PSA value after therapy, indirectly indicating a true positive finding. Thus, 38% of lesions assessed positive for LR remained unconfirmed.

Table 2 Comparison of findings and detection rate regarding local recurrence between early PET images and PET scans 60 min p.i. in patients subdivided in group 1, comprising all patients investigated ($n = 203$), and group 2, including only patients with absent urinary bladder activity ($n = 140$)

Local recurrence	Early PET group 1	PET 60 min group 1	*p* value*	Early PET group 2	PET 60 min group 2	*p* value*
Clearly negative	144	145	–	101	98	–
Equivocal	9	32	<0.001	0	23	<0.001
Clearly positive	50	26	<0.001	39	19	<0.001

*p value from McNemar test

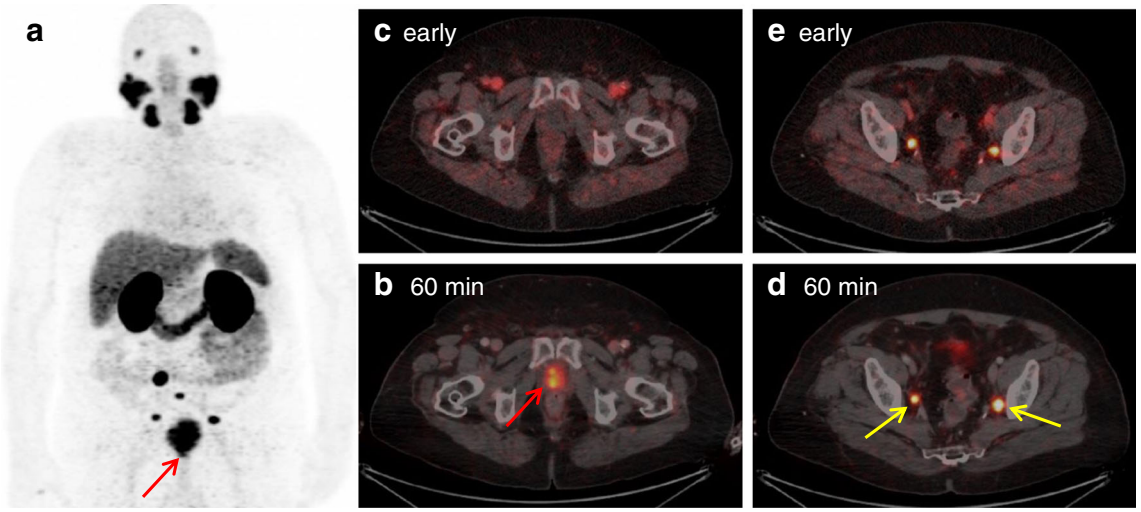

Fig. 2 ^{68}Ga-PSMA-11 PET/CT of a 62-year-old prostate cancer patient with biochemical relapse after radical prostatectomy (PSA at scan time: 1.5 ng/ml) with an equivocal finding in the prostatic fossa on images 60 min p.i., displayed on MIP (**a**) and fused PET/CT of the pelvis (**b**) with a *red arrow* pointing to the area of focal increased uptake. A clear distinction between local recurrence and urinary tracer activity is not possible. In contrast, on fused axial PET/CT images of early PET/CT (**c**), no pathologic tracer accumulation is found at that site, rendering a local recurrence unlikely. In addition, lymph nodes with intense tracer uptake in the pelvic area suggestive of metastases are seen on MIP with two of them marked on fused axial PET/CT images 60 min p.i. (**d**; *yellow arrow*), showing a clear correlate also on early PET/CT (**e**)

Discussion

According to the results of the first study published on biodistribution data of ^{68}Ga-PSMA-11 PET, whole-body PET acquisition is normally conducted 60 min p.i. in clinical practice [28]. However, intense physiologic urinary bladder accumulation, usually present at this time point, may obscure areas adjacent to the urinary bladder and may cause equivocal findings, especially with respect to evaluation of LR [21, 24, 29]. In addition, the so called "halo artefact" might also hamper assessment of areas in the vicinity of the urinary bladder. This phenomenon is well documented with ^{68}Ga-PSMA-11 PET/MRI studies [27]. It is caused by extinction of the PET signal due to high urinary bladder activity and was recently also described on ^{68}Ga-PSMA-11 PET/CT scans [21]. In fact, in our cohort, 26 patients (12.8%) did show a relevant halo artefact on PET scans 60 min p.i. Following the assumption that the lower the tracer activity in the urinary bladder, the better the visualization of PC lesions in sites close to the urinary bladder, several strategies which aim to reduce urinary bladder activity on PET scans 60 min p.i. are described [21, 29, 30]. Unfortunately, methods like administration of diuretics or catheterization of the urinary bladder show only limited success. Imaging at an early time point p.i., when urinary bladder activity is still not present, might also be a possible approach to solve this problem. In a study conducted by our group, we could show that early dynamic imaging allows differentiation of PC-related tracer uptake from activity in the urinary bladder in ^{68}Ga-PSMA-11 PET [25]. With early dynamic scans comprising the first 8 min p.i., we could demonstrate that ^{68}Ga-PSMA-11 uptake in lesions suggestive of PC occurs significantly earlier than tracer accumulation in the urinary bladder. PC lesions usually show a sufficient uptake of ^{68}Ga-PSMA-11 as early as 3–4 min p.i., whereas tracer accumulation in the urinary bladder is still absent in the vast majority of patients until 6 min p.i..

Although early dynamic imaging in ^{68}Ga-PSMA-11 PET is feasible, the applied imaging protocol is quite time-consuming

Table 3 Comparison of SUV_{max} values on early PET of lesions suggestive of local recurrence (n = 50) and reference tissues

	Median SUV_{max}	Mean SUV_{max}	SD SUV_{max}	Range SUV_{max}	p value*
LR, early PET	5.9	7.2	3.7	2.9–17.6	–
Seminal vesicle-anastomosis, early PET	2.4	2.4	0.4	1.1–3.6	<0.001
Gluteal muscle, early PET	1.9	2.0	0.4	1.1–3.3	<0.001
Inguinal vessel, early PET	4.0	4.1	1.0	1.9–7.0	<0.001

*p value from the Wilcoxon test for paired observations expressing differences of SUV_{max} values between LR and reference tissues on early PET

LR local recurrence

Table 4 Comparison of SUV_{max} values of all lesions suggestive of prostate cancer within pelvic area visible on both early PET and PET scans 60 min p.i. (local recurrence: $n = 26$; lymph nodes: $n = 82$; bone: $n = 27$), measured on early PET and 60 min p.i.

	Median SUV_{max}	Mean SUV_{max}	SD SUV_{max}	Range SUV_{max}	p value*
LR 60 min	10.8	15.2	10.3	4.7–40.9	<0.001
LR early PET	7.5	8.2	3.7	3.9–17.6	
LN 60 min	10.0	15.5	14.1	3.9–88.8	<0.001
LN early PET	7.8	10.3	7.7	2.9–46.2	
Bone 60 min	11.4	14.2	11.9	2.2–50.3	=0.002
Bone early PET	8.9	11.4	9.2	2.1–41.7	

*p value from the Wilcoxon test for paired observations testing differences between early PET and PET/CT after 60 min for LR, LN and bone

LR local recurrence, *LN* lymph node, *SD* standard deviation

and, in our experience, it is difficult to implement additional early dynamic scans of all PC patients as a standard in clinical routine, given limited PET scan resources. Therefore, the main purpose of this study was to assess if acquisition of a single early static image might constitute an alternative to early dynamic imaging and whether its use could improve the detection rate of LR in PC patients with BR. Kabasakal et al. already described the potential usefulness of early pelvic imaging with ^{68}Ga-PSMA-11 PET in PC patients [31]. They could not find a difference in the detection rate of LR between early images and PET scans 60 min p.i. As the inhomogeneous patient population of their study included only eight patients with BR, we tried to verify the value of early static imaging in a larger patient cohort, yielding more robust statistical data.

In a first step, we sought to determine which time point of acquisition start could be optimal for early static PET. Out of all 203 patients investigated, tracer accumulation in the urinary bladder was already present in 63 patients (31.0%) on early PET scans. However, the median acquisition starting time of patients without tracer activity in the urinary bladder was significantly lower in comparison to those patients with tracer accumulation already present in the urinary bladder (median time of acquisition start: 285 vs. 310 s; $p < 0.001$). In particular, almost all patients in whom acquisition was started in the fifth min p.i. did not show a relevant urinary bladder uptake. This goes in line with the data of the study on early dynamic imaging published by our group with urinary bladder activity appearing in most patients later than 6 min p.i. [25]. The differences in the time point of acquisition start are mostly attributable to the fact that we initially performed early imaging in the sixth to eighth min p.i. However, we soon realized that this might not be the ideal time point, as in a high number of patients, tracer activity in the urinary bladder had already occurred. Reinforced by the results of the study on early dynamic imaging, we decided to start image acquisition earlier thereafter. According to our findings, we suggest that acquisition of early static PET should start at the beginning of the fifth min p.i., in order to avoid disturbing urinary bladder activity on early static PET images. Also, for practical reasons, acquisition starting time 5 min p.i. has proven to be optimal, as tracer was not injected directly on the scanner with patients being positioned on the scanner only after tracer administration.

Although tracer accumulation in pathologic lesions including LR and metastases was significantly higher on PET scans 60 min p.i., tracer uptake of these lesions was found to be sufficient on early PET (see SUV_{max} measurements in Table 4). In particular, all lesions suggestive of LR on PET scans 60 min p.i. ($n = 26$) with a median SUV_{max} of 10.8 on images 60 min p.i. showed a good uptake also on early PET with a median SUV_{max} of 9.2. Importantly, no pathologic lesion consistent with LR on scans 60 min p.i. was missed on early PET. Only small LN metastases that were not distinguishable from surrounding iliac vessel activity and one small, purely sclerotic bone lesion could not be visualized on early PET. Tracer accumulation in all lesions suggestive of LR on early PET ($n = 50$) was significantly higher in comparison to physiologic inquinal vessel and gluteal muscle activity with a median SUV_{max} of 5.9, 4.0 and 1.9 respectively ($p < 0.001$). As the seminal vesicles and the vesicourethral anastomosis constitute the most common sites of LR, SUV_{max} of these areas was measured in patients with no apparent pathology at these regions, in order to exclude false positive interpretations due to blood pool activity. Again, the median SUV_{max} of LR-indicative lesions was significantly higher compared to this reference tissue (5.9 vs. 2.4; $p < 0.001$). Importantly, in contrast to inguinal vessel activity, the overlap in SUV_{max} values between normal anastomosis/seminal vesicles and malignant lesions was only small. Thus, we conclude that a focal tracer uptake present as early as 5 min p.i. at a LR-typical region most likely represents a finding consistent with PC lesion.

Applying this diagnostic criteria, we could identify LR-suggestive lesions in 50 out of 203 patients on early PET (24.6%) compared to findings judged positive for LR on PET scans 60 min p.i. in only 26 patients (12.8%), resulting in a significant increase of detection rate ($p < 0.001$).

The increase of detection rate was mostly due to a significant reduction of equivocal findings on early PET compared to PET scans 60 min p.i. In our experience, regions adjacent to the urinary bladder sometimes are difficult to assess on ^{68}Ga-PSMA-11 scans 60 min p.i. Unfortunately, these areas represent sites where local relapses in most of the patients occur. Especially, a focal uptake in the midline that cannot be clearly discriminated from urinary bladder activity represents a diagnostic challenge. We usually rate these findings as equivocal but not consistent with LR. Thus, the detection of LR may be underestimated on scans 60 min p.i. In fact, in this study, the number of uncertain cases was significantly reduced with the use of early PET in comparison to the scans 60 min p.i.

($p < 0.001$). Of note, the majority of equivocal findings 60 min p.i. were regarded as negative for LR on early PET, most likely representing urinary activity. Unclear findings were present in 32 patients (15.7%) on scans 60 min p.i., whereas only 9 patients (4.4%) were described as equivocal for LR on early images. The benefit was even more pronounced in the subgroup of patients without urinary tracer activity on early PET ($n = 140$) with no equivocal finding on early PET compared to 23 uncertain cases on PET images 60 min p.i. (16.4%).

Interestingly, patients with lower PSA values were more likely to show LR visible only on early PET. In contrast, patients with higher PSA levels tended to be judged positive on both early PET and PET scans 60 min p.i. (median PSA: 2.02 vs. 4.59 ng/ml). As serum PSA usually reflects tumour volume, the difference might be attributed to a smaller tumour size of LR that could not be discernable on PET scans 60 min p.i. at sites adjacent to the urinary bladder.

Briefly, the overall rate of PET positivity with 62.1% of patients showing at least one pathologic lesion seems relatively low compared to other studies published to date [20, 32–35]. This might be due to the comparatively low PSA values of the patient population (median PSA: 1.44 ng/ml), including a quite high number of patients with a PSA level <1.0 and <0.5 ng/ml (35.5% and 20.2% of patients, respectively).

One major limitation of the study is the fact that pathologic findings regarding LR could only be verified in 62% of patients. In particular, histologic confirmation was not obtained in any of the patients, partly due to practical reasons, as in patients who underwent salvage radiotherapy thereafter the decision was solely based on imaging results. However, the data of early imaging are quite consistent. All lesions rated clearly positive for LR on scans 60 min p.i. could also be seen on early images. This goes in line with the results of our previous study on early dynamic imaging. A focal tracer uptake in the prostatic fossa, which is visible prior to tracer accumulation in the urinary bladder, is highly suspicious of LR [25]. In addition, all pathologic lesions rated as metastases in the pelvic area on scans 60 min p.i. were also found on early PET images, apart from some LN that were obscured by iliacal vessel activity. Therefore, it seems very likely that a focal tracer accumulation at LR-typical sites on early static scans could be considered as a true positive finding too, as long as there is no tracer activity visible in the urinary bladder. Nevertheless, we acknowledge the fact that efforts have to be made that these encouraging results of early PET need to be confirmed in further studies with histology results as the reference standard.

Conclusions

In this study, we could demonstrate that application of early static scans of the pelvis enhances the detection rate of local relapse in PC patients with BR referred to ^{68}Ga-PSMA-11 PET/CT. It particularly seems to represent a powerful method in clarifying equivocal findings on PET scans 60 min p.i. in areas adjacent to the urinary bladder. With acquisition starting at the beginning of the fifth min p.i., no urinary bladder activity is present in the majority of patients on early PET images, whereas PC-related tumour lesions already show a sufficient high tracer uptake at this time point. Therefore, we advise integrating early static PET imaging in the standard acquisition protocol of ^{68}Ga-PSMA-11 PET/CT for PC patients with biochemical relapse.

Acknowledgements We want to express our gratitude to all the members of our PET staff for their contribution in performing this study.

Compliance with ethical standards

Conflict of interest All authors declare that they have no conflicts of interest.

Ethical approval All procedures performed in this study were in accordance with the ethical standards of the institutional and national research committee and with the principles of the 1964 Declaration of Helsinki and its subsequent amendments [36]. All patients of whom data was published in this manuscript signed a written informed consent.

References

1. Mottet N, Bellmunt J, Bolla M, Briers E, Cumberbatch MG, De Santis M, et al. EAU-ESTRO-SIOG guidelines on prostate cancer. Part 1: Screening, diagnosis, and local treatment with curative intent. Eur Urol. 2016.
2. Mullins JK, Feng Z, Trock BJ, Epstein JI, Walsh PC, Loeb S. The impact of anatomical radical retropubic prostatectomy on cancer control: the 30-year anniversary. J Urol. 2012;188(6):2219–24.
3. Amling CL, Bergstralh EJ, Blute ML, Slezak JM, Zincke H. Defining prostate specific antigen progression after radical prostatectomy: what is the most appropriate cut point? J Urol. 2001;165(4):1146–51.
4. Cornford P, Bellmunt J, Bolla M, Briers E, De Santis M, Gross T, et al. EAU-ESTRO-SIOG guidelines on prostate cancer. Part II: Treatment of relapsing, metastatic, and castration-resistant prostate cancer. Eur Urol. 2016.
5. Rouvière O, Vitry T, Lyonnet D. Imaging of prostate cancer local recurrences: why and how? Eur Radiol. 2010;20(5):1254–66.
6. Beresford MJ, Gillatt D, Benson RJ, Ajithkumar T. A systematic review of the role of imaging before salvage radiotherapy for post-prostatectomy biochemical recurrence. Clin Oncol (R Coll Radiol). 2010;22(1):46–55.
7. Pfister D, Bolla M, Briganti A, Carroll P, Cozzarini C, Joniau S, et al. Early salvage radiotherapy following radical prostatectomy. Eur Urol. 2014;65(6):1034–43.
8. De Visschere PJ, De Meerleer GO, Fütterer JJ, Villeirs GM. Role of MRI in follow-up after focal therapy for prostate carcinoma. AJR am J Roentgenol. 2010;194(6):1427–33.
9. Picchio M, Briganti A, Fanti S, Heidenreich A, Krause BJ, Messa C, et al. The role of choline positron emission tomography/computed tomography in the management of patients with prostate-specific antigen progression after radical treatment of prostate cancer. Eur Urol. 2011;59(1):51–60.

10. Evangelista L, Cimitan M, Hodolič M, Baseric T, Fettich J, Borsatti E. The ability of 18F-choline PET/CT to identify local recurrence of prostate cancer. Abdom Imaging. 2015;40(8):3230–7.
11. Fanti S, Minozzi S, Castellucci P, Balduzzi S, Herrmann K, Krause BJ, et al. PET/CT with (11)C-choline for evaluation of prostate cancer patients with biochemical recurrence: meta-analysis and critical review of available data. Eur J Nucl med Mol Imaging. 2016;43(1):55–69.
12. Panebianco V, Sciarra A, Lisi D, Galati F, Buonocore V, Catalano C, et al. Prostate cancer: 1HMRS-DCEMR at 3T versus [(18)F]choline PET/CT in the detection of local prostate cancer recurrence in men with biochemical progression after radical retropubic prostatectomy (RRP). Eur J Radiol. 2012;81(4):700–8.
13. Kitajima K, Murphy RC, Nathan MA, Froemming AT, Hagen CE, Takahashi N, et al. Detection of recurrent prostate cancer after radical prostatectomy: comparison of 11C-choline PET/CT with pelvic multiparametric MR imaging with endorectal coil. J Nucl med. 2014;55(2):223–32.
14. Ceci F, Herrmann K, Castellucci P, Graziani T, Bluemel C, Schiavina R, et al. Impact of 11C-choline PET/CT on clinical decision making in recurrent prostate cancer: results from a retrospective two-centre trial. Eur J Nucl med Mol Imaging. 2014;41(12):2222–31.
15. Eiber M, Maurer T, Souvatzoglou M, Beer AJ, Ruffani A, Haller B, et al. Evaluation of hybrid ^{68}Ga-PSMA ligand PET/CT in 248 patients with biochemical recurrence after radical prostatectomy. J Nucl med. 2015;56(5):668–74.
16. Ceci F, Uprimny C, Nilica B, Geraldo L, Kendler D, Kroiss A, et al. (68)Ga-PSMA PET/CT for restaging recurrent prostate cancer: which factors are associated with PET/CT detection rate? Eur J Nucl med Mol Imaging. 2015;42(8):1284–94.
17. Afshar-Oromieh A, Avtzi E, Giesel FL, Holland-Letz T, Linhart HG, Eder M, et al. The diagnostic value of PET/CT imaging with the (68)Ga-labelled PSMA ligand HBED-CC in the diagnosis of recurrent prostate cancer. Eur J Nucl med Mol Imaging. 2015;42(2):197–209.
18. Afshar-Oromieh A, Haberkorn U, Eder M, Eisenhut M. Zechmann CM.[68Ga]gallium-labelled PSMA ligand as superior PET tracer for the diagnosis of prostate cancer: comparison with 18F-FECH. Eur J Nucl med Mol Imaging. 2012;39(6):1085–6.
19. Afshar-Oromieh A, Zechmann CM, Malcher A, Eder M, Eisenhut M, Linhart HG, et al. Comparison of PET imaging with a (68)Ga-labelled PSMA ligand and (18)F-choline-based PET/CT for the diagnosis of recurrent prostate cancer. Eur J Nucl med Mol Imaging. 2014;41(1):11–20.
20. Morigi JJ, Stricker PD, van Leeuwen PJ, Tang R, Ho B, Nguyen Q, et al. Prospective comparison of 18F-Fluoromethylcholine versus 68Ga-PSMA PET/CT in prostate cancer patients who have rising PSA after curative treatment and are being considered for targeted therapy. J Nucl med. 2015;56(8):1185–90.
21. Rauscher I, Maurer T, Fendler WP, Sommer WH, Schwaiger M, Eiber M. (68)Ga-PSMA ligand PET/CT in patients with prostate cancer: how we review and report. Cancer Imaging. 2016;16(1):14.
22. Afshar-Oromieh A, Hetzheim H, Kübler W, Kratochwil C, Giesel FL, Hope TA, et al. Radiation dosimetry of (68)Ga-PSMA-11 (HBED-CC) and preliminary evaluation of optimal imaging timing. Eur J Nucl med Mol Imaging. 2016;43(9):1611–20.
23. Demirci E, Sahin OE, Ocak M, Akovali B, Nematyazar J, Kabasakal L. Normal distribution pattern and physiological variants of 68Ga-PSMA-11 PET/CT imaging. Nucl med Commun. 2016;37(11):1169–79.
24. Freitag MT, Radtke JP, Afshar-Oromieh A, Roethke MC, Hadaschik BA, Gleave M, et al. Local recurrence of prostate cancer after radical prostatectomy is at risk to be missed in ⁶⁸Ga-PSMA-11-PET of PET/CT and PET/MRI: comparison with mpMRI integrated in simultaneous PET/MRI. Eur J Nucl med Mol Imaging. 2017;44(5):776–87.
25. Uprimny C, Kroiss AS, Decristoforo C, Fritz J, Warwitz B, Scarpa L, et al. Early dynamic imaging in ^{68}Ga- PSMA-11 PET/CT allows discrimination of urinary bladder activity and prostate cancer lesions. Eur J Nucl Med Mol Imaging. 2016.
26. Uprimny C, Kroiss AS, Decristoforo C, Fritz J, von Guggenberg E, Kendler D, et al. ^{68}Ga-PSMA-11 PET/CT in primary staging of prostate cancer: PSA and Gleason score predict the intensity of tracer accumulation in the primary tumour. Eur J Nucl Med Mol Imaging. 2017.
27. Noto B, Büther F, Auf der Springe K, Avramovic N, Heindel W, Schäfers M, et al. Impact of PET acquisition durations on image quality and lesion detectability in whole-body 68Ga-PSMA PET-MRI. EJNMMI res. 2017;7(1):12.
28. Afshar-Oromieh A, Malcher A, Eder M, Eisenhut M, Linhart HG, Hadaschik BA, et al. PET imaging with a [68Ga]gallium-labelled PSMA ligand for the diagnosis of prostate cancer: biodistribution in humans and first evaluation of tumour lesions. Eur J Nucl med Mol Imaging. 2013;40(4):486–95.
29. Afshar-Oromieh A, Sattler LP, Mier W, Hadaschik B, Debus J, et al. The clinical impact of additional late PET/CT imaging with 68Ga-PSMA-11 (HBED-CC) in the diagnosis of prostate cancer. J Nucl Med. 2017.
30. Derlin T, Weiberg D, von Klot C, Wester HJ, Henkenberens C, Ross TL, et al. 68Ga-PSMA I&T PET/CT for assessment of prostate cancer: evaluation of image quality after forced diuresis and delayed imaging. Eur Radiol. 2016;26(12):4345–53.
31. Kabasakal L, Demirci E, Ocak M, Akyel R, Nematyazar J, Aygun A, et al. Evaluation of PSMA PET/CT imaging using a 68Ga-HBED-CC ligand in patients with prostate cancer and the value of early pelvic imaging. Nucl med Commun. 2015;36(6):582–7.
32. van Leeuwen PJ, Stricker P, Hruby G, Kneebone A, Ting F, Thompson B, et al. (68) Ga-PSMA has a high detection rate of prostate cancer recurrence outside the prostatic fossa in patients being considered for salvage radiation treatment. BJU Int. 2016;117(5):732–9.
33. Verburg FA, Pfister D, Heidenreich A, Vogg A, Drude NI, Vöö S, et al. Extent of disease in recurrent prostate cancer determined by [(68)Ga]PSMA-HBED-CC PET/CT in relation to PSA levels, PSA doubling time and Gleason score. Eur J Nucl med Mol Imaging. 2016;43(3):397–403.
34. Sterzing F, Kratochwil C, Fiedler H, Katayama S, Habl G, Kopka K, et al. (68)Ga-PSMA-11 PET/CT: a new technique with high potential for the radiotherapeutic management of prostate cancer patients. Eur J Nucl med Mol Imaging. 2016;43(1):34–41.
35. Perera M, Papa N, Christidis D, Wetherell D, Hofman MS, Murphy DG, et al. Sensitivity, specificity, and predictors of positive 68Ga-prostate-specific membrane antigen positron emission tomography in advanced prostate cancer: a systematic review and meta-analysis. Eur Urol. 2016;70(6):926–37.
36. World Medical Association Declaration of Helsinki: ethical principles for medical research involving human subjects. JAMA. 2000;284:3043–5.